RAPID COMMUNICATIONS

PHYSICAL REVIEW A VOLUME 42, NUMBER 5 1 SEPTEMBER 1990

Ionization of atoms in intense laser pulses using the Kramers-Henneberger transformation

V. C. Reed and K. Burnett

Clarendon Laboratory, Department of Physics, University of Oxford, Parks Road, Oxford OX1 3PU, United Kingdom

(Received 7 May 1990; revised manuscript received 29 June 1990)

We present a general technique for the numerical calculation of the behavior of an electron in an intense laser field, by the direct integration of the time-dependent Schrödinger equation in the Kramers-Henneberger frame. We give results for a model potential; these include above-threshold ionization spectra for the transition regime to over-the-barrier escape. We also show how satellite spectra can develop in long pulses.

The most direct method of studying the effect of intense laser fields on atoms is to integrate the time-dependent Schrödinger equation. A time-domain approach is also necessary if one wants to model present experiments that involve laser pulses of typically a hundred femtosecond duration.[1] We shall present what we believe is an improved method of calculation using the time-dependent Schrödinger equation that allows us to examine the behavior of atoms in realistic pulses without the use of extremely large amounts of computer time. Such a calculation also offers the possibility of producing above-threshold ionization (ATI) spectra at higher intensities than was previously possible.

The basis of our technique involves the integration of the time-dependent Schrödinger equation in the Kramers-Henneberger (KH) frame,[2,3] the use of this frame being crucial in the reduction of computer time needed. The KH frame is the frame of motion of a free electron in the applied laser field and previous work has shown how this frame can be used to good effect in Floquet calculations for constant amplitude fields.[4] The frame has also been used to interpret the results of previous time-dependent calculations.[5] We have performed the first time-dependent calculation that directly uses this frame, by doing so we take advantage of the fact that a wave packet quickly becomes free in this frame, as we explain below.

The wave functions in the laboratory (lab) and Kramers-Henneberger (KH) frames are related by a unitary transformation:

$$\phi_{\mathrm{KH}}(\mathbf{r},t)=U_1U_2\psi_{\mathrm{lab}}(\mathbf{r},t)\,, \tag{1}$$

where

$$U_1=\exp\left[\frac{iq^2}{2m\hbar}\int_{-\infty}^{t}d\tau\mathbf{A}^2(\tau)\right], \tag{2}$$

$$U_2=\exp\left[\frac{-q}{m}\int_{-\infty}^{t}d\tau\mathbf{A}(\tau)\cdot\nabla\right]. \tag{3}$$

U_1 is a phase-transformation operator that removes the $\mathbf{A}^2$ term from the Schrödinger equation and U_2 represents a shift to the accelerated frame of reference. The application of the KH transformation to the $\mathbf{p}\cdot\mathbf{A}$ gauge Schrödinger equation results in the transformed wave function satisfying the following differential equation:

$$i\hbar\frac{\partial\phi_{\mathrm{KH}}(\mathbf{r},t)}{\partial t}=\left[-\frac{\hbar^2}{2m}\nabla^2+V(\mathbf{r}+\boldsymbol{\alpha}(t))\right]\phi_{\mathrm{KH}}(\mathbf{r},t)\,, \tag{4}$$

where

$$\boldsymbol{\alpha}(t)=-\frac{q}{m}\int_{-\infty}^{t}\mathbf{A}(\tau)d\tau\,. \tag{5}$$

In this representation of the Schrödinger equation the applied electric field appears only in the time-dependent part of the potential. So in the KH frame the effect of the laser field on an escaping electron wave packet during the ionization process decreases as the effect of the potential decreases. Hence, once an electron passes beyond the range of the potential it can be described as a free-electron wave packet. This allows us to perform pulse calculations of realistic length with much greater ease than if we were working in the laboratory frame. In the laboratory frame, the length of pulse that can be used is restricted by the dimensions of the space grid. Once an electron wave packet has reached the edge of the grid, the calculation must stop to prevent the wave packet back-propagating and interacting with the field. In the KH frame, however, since the effect of our field is localized, the wave packets at the edge of the grid are free and they can be allowed to reflect back from the boundary and propagate back towards the core until such a time as the fastest moving wave packet begins to interact with the core again; this allows a smaller grid to be used.

In our calculation the field is treated classically within the dipole approximation as a monochromatic infinite plane wave. The effect of the pulse length, and shape of the pulse envelope, can be readily modeled by the appropriate variation of the time-dependent parameter $\boldsymbol{\alpha}(t)$. The calculation we present here is for a one-dimensional potential, which makes the calculations particularly rapid. The technique is, of course, not limited to one dimension. The initial state in the calculation is a bound state of the zero-field potential, with boundary conditions being imposed by the edge of the grid. The time evolution is performed in the KH frame using a standard Crank-Nicholson finite-difference iterative method.[6] At the end of the evolution, the free-electron energy spectrum is calculated by transforming the evolved wave function back to the $\mathbf{d}\cdot\mathbf{E}$ frame and then overlapping with the zero-field

positive energy eigenfunctions. A Convex C120 vector processor is used for the calculation, which operates, for our routines, at approximately one-eighth the speed of a Cray 1S computer. Further details of the calculation are planned to be published.

The general method of calculation is applicable to any potential but for the results that we present here, we have used the potential

$$V(x)=\frac{-1}{\sqrt{1+x^2}}. \tag{6}$$

This has the advantage that it has a Coulomb tail and hence gives a high-lying Rydberg series, with parity as a good quantum number. In addition, it is the same potential that was used by Javanainen *et al.*,[7] which enables us to directly compare our results with theirs. When calculations are performed using the same parameters as those of Javanainen *et al.*,[7] exactly identical ATI spectra are obtained with considerably smaller and coarser grids and larger time steps.

The pulse envelope used has an electric field given by

$$E(t)=E_0\sin^2\left(\frac{\pi t}{T}\right)\sin(\omega t), \tag{7}$$

where T is the pulse length. Because of the smooth turn-on of the field, fewer harmonics of the field are present and so the population of the atom remains initially in the ground state and is not immediately elevated to the higher bound states. We have taken advantage of the reduction in CPU time afforded us by the use of the KH frame and have performed calculations for pulse lengths that are used at present in experiments. Figures 1(a) and 1(b) show typical results from our calculations where the parameters used correspond to those of a Kr-F laser with pulse lengths of 53 and 200 fs. There is good agreement of the peak positions with those predicted by the formula for the free-electron energy, $\varepsilon_f=\varepsilon_g(I)+n\omega-\varepsilon_i(I)$, where $\varepsilon_g(I)$ is the ground-state energy, which is negligibly shifted in the intensity range of our calculations, n is the number of photons absorbed and $\varepsilon_i(I)$ is the ionization potential of the atom.

In addition to the main peaks, numerous satellite peaks are observable on the high-energy side. These "rainbow" features can be interpreted as being due to the quantum-mechanical interference of the waves produced at the same electric field on the rising and falling edge of the pulse.[8,9] The largest amount of ionization which gives the main peak occurs at the peak electric field when the field is slowly varying. A simple model to explain this effect assumes that the translational energy of the ionized electron can be written as

$$\varepsilon(t)=\varepsilon_0+n\omega+\alpha t^2-E_0^2/4\omega^2. \tag{8}$$

Stationary phase analysis of the continuum amplitude calculated using the above expression predicts minima at the following energies:

$$\varepsilon_{\min}(t)=\varepsilon_0+n\omega-\frac{E_0^2}{4\omega^2}+f(E_0)\frac{(2n+1)^{2/3}}{N^{2/3}}, \tag{9}$$

where $f(E_0)$ is some function of peak electric field, N is the number of cycles of the laser field in the pulse, and

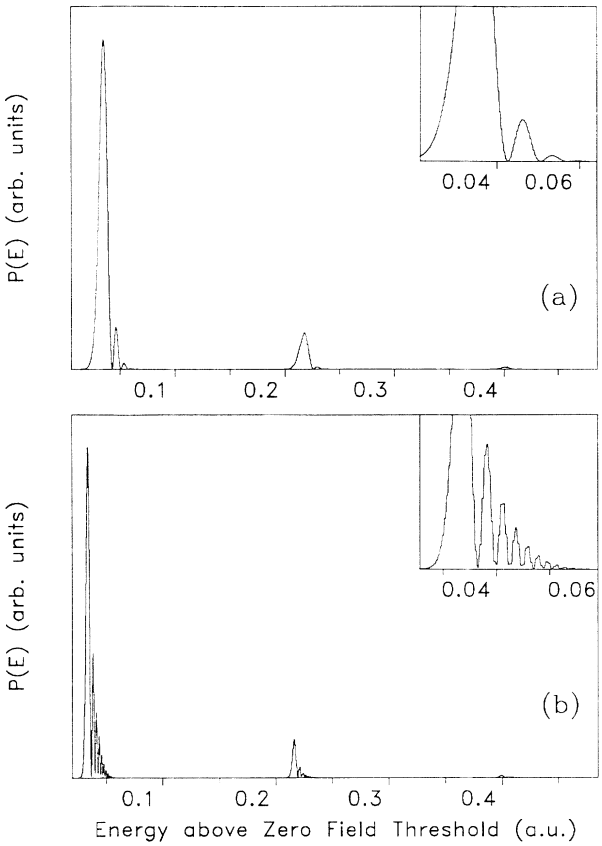

FIG. 1. Electron spectra for (a) 53- and (b) 200-fs pulses. The parameters used correspond to those of a Kr-F laser, with $\lambda=0.25$ μm and intensity $=10^{14}$ W/cm^2. The calculations used 16 384 grid points at a grid spacing of $\Delta x=0.2$ and 150 time steps per cycle of the laser field and took approximately 50 min and 3 h of CPU time, respectively. The insets show the detailed satellite peaks of the first ATI peaks.

$n=0,1,2,\ldots$. Analysis of the minima of the subpeaks of Figs. 1(a) and 1(b) give results that closely agree with those predicted by Eq. (9). The fine detail of these oscillations will, of course, be affected by spatial averaging in a real experiment. We are at present undertaking a detailed study of the formation of the satellite peaks for various pulse shapes.

Using the same pulse shape, the effect of increasing the laser intensity has been studied. Figures 2(a)–2(d) show the effect of increasing the intensity from 10^{14} to 5×10^{15} W/cm^2. Multiphoton ionization (MPI) is not the only process by which electrons can escape.[10] As the electric field increases, the potential barrier at the maximum field becomes thinner and tunneling can occur. Also at higher fields, the top of the potential barrier can be below the ground state and provided that the laser frequency is small compared to the atomic frequency, the electron can pass over the barrier and ionize. Unlike MPI and tunneling ionization, escape over the barrier does not produce peaks in the energy spectrum because of the short lifetime of the bound state. An estimate of when over-the-barrier (OTB) ionization can occur can be obtained using a static field approximation and it yields the result that OTB ionization can occur when the electric field E is such that

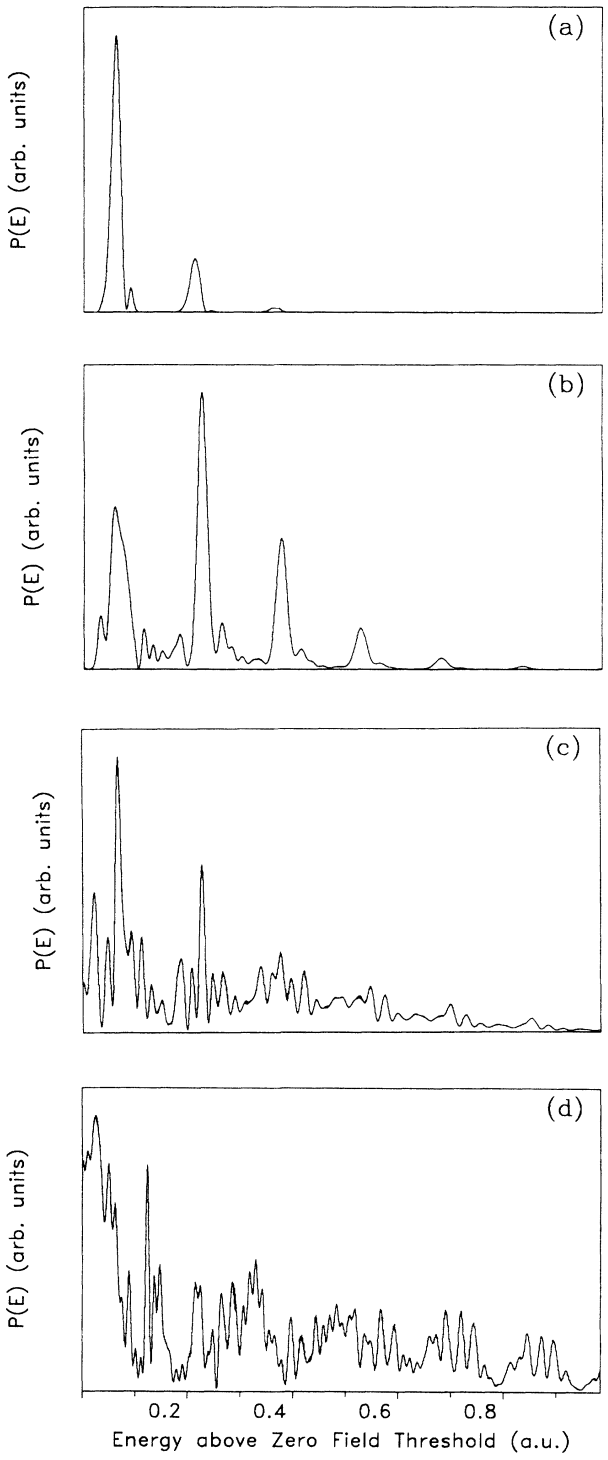

FIG. 2. Electron spectra for 20-fs pulses at a wave length of $\lambda = 300$ nm. 16384 grid points at a grid spacing of $\Delta x = 0.2$ were used, with 150 times steps per laser cycle. The calculations were performed in approximately 30 min. The intensities used are (a) 10^{14} W/cm^2, (b) 5×10^{14} W/cm^2, (c) 10^{15} W/cm^2, and (d) 5×10^{15} W/cm^2.

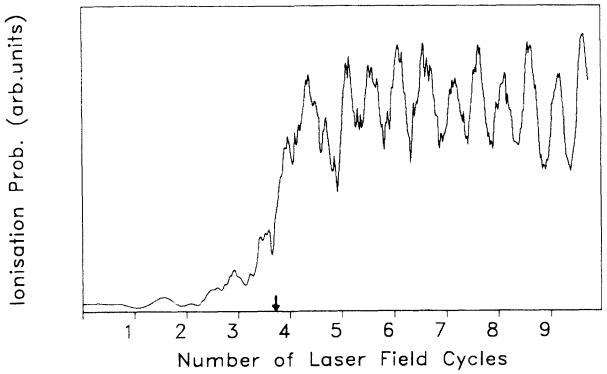

FIG. 3. Ionization probability as a function of time for the parameters of Fig. 2(d). The curve has been smoothed over the fast oscillations of the probability and the arrow indicates where OTB ionization becomes possible. The total ionization after half the pulse is 0.803.

$2E^{1/2} \geq \varepsilon_g$, the ground-state energy. For our potential, $E \geq 0.112$. Figures 2(a)–2(d) illustrate this condition. In Fig. 2(a), the electric field is never big enough for OTB ionization to occur, so the ATI peaks are well defined against the background. For the higher intensity in Fig. 2(b), OTB ionization can only occur close to the field maximum and so the background in the energy spectrum is only slightly increased compared to Fig. 1. In Fig. 2(c), however, OTB ionization can occur for nearly 8 cycles of the field and the background in the energy spectrum due to the OTB ionization is comparable to the ATI peaks. In Fig. 2(d), OTB ionization has become the dominant method and no ATI peaks are discernible. Very little MPI has occurred and at about 3.7 cycles of the field, OTB ionization is possible and the wave function rapidly escapes. This is further illustrated in Fig. 3 by the plot of ionization probability as a function of time for the parameters of Fig. 2(d). There is a gradual rise in ionization due to MPI until 3.7 cycles when there is sharp increase as OTB ionization becomes possible.

In conclusion, the general technique outlined above opens the way to performing a large range of calculations for realistic length pulses. The speed of the computation will be increased further by developments we have planned on more efficient wave-packet propagation. We believe this will open the way to very rapid long pulse one-dimensional calculations, using only minutes of CPU time, and also to long pulse two-dimensional calculations. Such calculations will play an important part in examining the role of pulse shape and other time-dependent phenomena on the behavior of atoms in intense fields.

We thank Dr. S. M. Barnett and Dr. B. R. M. Piraux and Professor P. L. Knight for helpful discussions. V.C.R. acknowledges the support of United Kingdom Science and Engineering Research Council (SERC) and STC Technology limited.

[1]P. Agostini, A. Antonetti, P. Breger, M. Crance, A. Migus, H. G. Muller, and G. Petite, J. Phys. B **22**, 1971 (1989).

[2]H. A. Kramers, *Collected Scientific Papers* (North-Holland, Amsterdam, 1956), p. 272.

[3]W. C. Henneberger, Phys. Rev. Lett. **21**, 838 (1968).

[4]R. Bhatt, B. Piraux, and K. Burnett, Phys. Rev. A **37**, 98 (1988).

[5]M. Gavrila and J. Z. Kaminski, Phys. Rev. Lett. **52**, 613 (1984).

[6]W. H. Press, B. P. Flannery, S. A. Teukolsky, and W. T. Vetterling, *Numerical Recipes* (Cambridge Univ. Press, Cambridge, England, 1987).

[7]J. Javanainen, J. H. Eberly, and Qichang Su, Phys. Rev. A **38**, 3430 (1988).

[8]M. A. Lauder, P. Knight, and P. T. Greenland, Optica Acta **33**, 1231 (1986), and references therein.

[9]J. N. Bardsley, A. Szöke, and M. J. Comella, J. Phys. B **21**, 3899 (1988).

[10]S. Geltman, J. Phys. B **10**, 831 (1977).